JOURNAL OF AIRCRAFT
Vol. 30, No. 4, July–Aug. 1993

Effect of Stiffness Characteristics on the Response of Composite Grid-Stiffened Structures

Damodar R. Ambur*
NASA Langley Research Center, Hampton, Virginia 23665
and
Lawrence W. Rehfield†
University of California, Davis, Davis, California 95616

A study of the effect of stiffness discontinuities and structural parameters on the response of continuous-filament grid-stiffened flat panels is presented. The buckling load degradation due to manufacturing-introduced stiffener discontinuities associated with a filament cut-and-add approach at the stiffener intersections is investigated. For practical discontinuity sizes, the reduction in buckling load is negligible. The degradation of buckling resistance in isogrid flat panels subjected to uniaxial compression, combined axial compression, shear loading conditions, and induced damage, is quantified using finite element analysis. The combined loading case is the most critical one. The benefit of utilizing nonsolid stiffener cross sections is evaluated. Nonsolid stiffener cross sections, such as a foam-filled blade or hat with a 0-deg dominant cap, result in grid-stiffened structures that are structurally very efficient for wing and fuselage applications. The results of a study of the ability of grid-stiffened structural concepts to enhance the effective Poisson's ratio of a panel is presented. Grid-stiffened concepts create a high effective Poisson's ratio which can produce large camber deformations for certain elastic tailoring applications.

Introduction

STRUCTURAL efficiency is an important aspect of the design of cost-effective aircraft structures. This efficiency requirement is accomplished in most instances through the increased use of stiffened composite structures that consist of flat or curved panels that are reinforced by stiffeners. These stiffeners are either cocured, bonded, or bolted to the panel. (In a cocuring process, the stiffener and skin are cured together to result in a stiffened panel.) Of these attachment concepts, stiffened composite structures produced by cocuring are the most cost effective due to reduced part count. Although many manufacturing processes are available to produce cocured structures, automated tow or tape placement and filament or tape winding methods have emerged as some of the most viable ones.

The continuous-filament grid-stiffened structures are produced by winding or laying continuous filaments in an automated process. Different structural configurations like orthogrid (stiffeners placed in mutually perpendicular directions), isogrid (stiffeners placed in an equilateral triangular pattern), or any general grid (stiffeners placed in arbitrary directions) may be produced using this manufacturing process. The continuous-filament isogrid structure was first produced in 1976 in an effort to develop efficient, low-cost structures. The compressive buckling and dynamic behavior of this isogrid structural concept were studied in Refs. 1–3. The damage tolerance of this structural concept when subjected to uniaxial compression was demonstrated experimentally, and verified with finite element results.[4,5] A design study conducted on a Lockheed C-130 transport aircraft center fuselage using continuous-filament grid-stiffened concepts, like isogrid and orthogrid, demonstrated a weight savings of 20–30% over the conventional metallic design.[6] In a recent study, structural analysis and design optimization of a geodesically stiffened wing rib panel was performed.[7] The tail-boom of Bell Helicopter Textron's Advanced Composite Airframe Program candidate has a grid-type construction reinforced by fiberglass-epoxy/polyamide-foam sandwich longerons.[8] Although there have been many studies and applications involving continuous filament grid-stiffened structures as summarized above, several aspects of this promising structural concept remain to be investigated.

The objective of this article is to present the results of the effects of stiffness discontinuities and selected structural parameters on the behavior of grid-stiffened panels. Specifically, the effects of both manufacturing-introduced stiffness discontinuities and induced damage on grid-stiffened panel buckling behavior are addressed herein. In an effort to avoid filament clustering at the stiffener intersections, several new manufacturing methods have been proposed. One such proposed method is the tape cut-and-add approach. A detailed view of a stiffener discontinuity that results at the stiffener intersection in an orthogrid panel due to the tape cut-and-add approach is shown in Fig. 1. In the cut-and-add manufacturing method, the tape from stiffener 1 approaching the intersection is cut before the intersection and added after the intersection. This process leaves a gap at the intersection that is larger than the tape width, which permits the tape at the corresponding height in stiffener 2 to pass through the intersection. In the adjacent layer (immediately above or below the previous one) the tape in stiffener 2 is cut and added while the tape in stiffener 1 passes through the intersection. This approach avoids fiber clustering at the stiffener intersection that results from passing all filament tapes in stiffeners 1 and 2 through the intersection. Such fiber clustering has been found to considerably reduce the stiffness and strength of the intersection regions (Ref. 2). The cut-and-add approach is beneficial since the filaments remain straight through the stiffener intersection. However, since a stiffness discontinuity results at the intersection, this region has reduced mechanical properties

Received Feb. 19, 1991; presented as Paper 91-1087 at the AIAA/ASME/ASCE/AHS 32nd Structures, Structural Dynamics, and Materials Conference, Baltimore, MD, April 8–10, 1991; revision received April 27, 1992; accepted for publication May 21, 1992.

*Aerospace Engineer, Aircraft Structures Branch, Structural Mechanics Division. Member AIAA.
†Professor, Division of Aeronautical Sciences and Engineering. Associate Fellow AIAA.

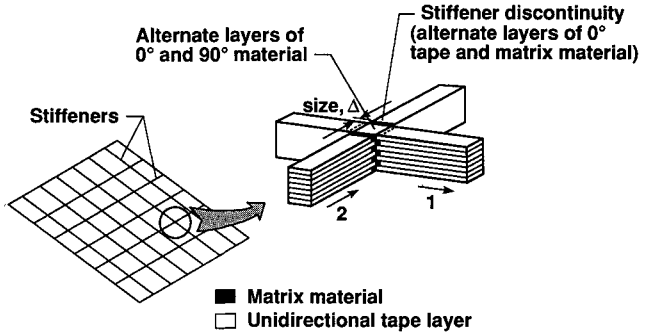

Fig. 1 Details of stiffener discontinuity in an orthogrid panel fabricated by the cut-and-add approach.

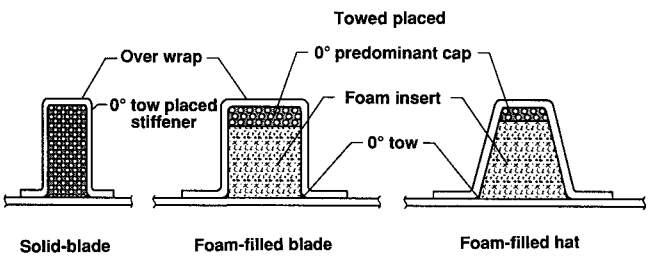

Fig. 2 Stiffener cross sections.

compared to the rest of the stiffener. Depending on the size of this discontinuity, the buckling resistance of the grid-stiffened structure could degrade considerably. This reduction in buckling resistance needs to be evaluated before accepting the cut-and-add approach as a practical method of manufacturing.

The buckling behavior of orthogrid panels with stiffness discontinuities due to the cut-and-add manufacturing approach is investigated in the present article. The tolerance of grid stiffened structures to induced damage is considered an inherent feature, as the structure has a multiplicity of load paths. This damage-tolerant behavior is demonstrated to a limited extent in Refs. 4 and 5 for a wide column structural application. The damage tolerance information for grid-stiffened panels with more practical boundary conditions and general in-plane loading conditions is lacking. Thus, the damage tolerant characteristics of simply-supported isogrid panels subjected to different loading conditions are evaluated in this article.

Also, the improved benefits from grid-stiffened structures obtained by suitably designing structural parameters such as stiffener cross section and stiffener orientation to the primary load direction are addressed in this article. In the work conducted so far on grid-stiffened structures, only solid rectangular (blade) sections shown in Fig. 2 have been used for the stiffeners. Other stiffener cross sections such as the foam-filled blade and the foam-filled hat that are proposed in this article need to be evaluated to identify more promising structural concepts. Typical construction details of these cross sections are shown in Fig. 2. The structural efficiencies of panels with these new, alternative cross sections are investigated in the present article. One way to elastically tailor a structure is to orient the stiffeners suitably with respect to the primary load direction to derive the most desirable response. Grid-stiffened concepts are particularly useful for elastic tailoring of structures because stiffeners made of unidirectional material can be oriented to create a wide variation of elastic properties. For one high-aspect ratio wing concept, a large effective Poisson's ratio is desired for the wing covers to produce chordwise camber deformations. The application of a grid-stiffened concept to provide enhancements in the effective Poisson's ratio and, hence, large camber deformations is discussed herein.

Analysis and Discussion of Results

Effect of Stiffness Discontinuities

Two types of stiffness discontinuities are considered in this study. One type is a manufacturing-introduced stiffness discontinuity at the stiffener intersections due to a cut-and-add approach used during fabrication. The second type is due to induced damage to the stiffener elements of the grid-stiffened panel. The buckling response of grid-stiffened panels with the above types of stiffness discontinuities is discussed in the following paragraphs.

Effect of Manufacturing Introduced Stiffness Discontinuities on Orthogrid Panel

The orthogrid panel considered for evaluation with the above stiffener discontinuities is designed to carry a combined axial compression, shear, and transverse tensile loading of 525 kN/m (3000 lb/in.), 105 kN/m (600 lb/in.), and 263 kN/m (1500 lb/in.), respectively, that is representative of transport fuselage loading. The material system chosen for design is Hercules AS4/3501-6 graphite-epoxy material with typical properties shown in Table 1. The use of trademarks or manufacturer's names in this article does not constitute endorsement, either expressed or implied, by NASA. A detailed model with the exact representation of each intersection point using five regions (one region to represent the 0-/90-deg material at the center of the intersection and four regions of 0 deg-fiber/matrix-layer material to represent the stiffener discontinuities around the central region as shown in Fig. 1) results in a large finite element model. A relatively smaller model can be developed by using one region to represent each of the intersection points that has smeared constitutive properties of the above five regions to estimate the changes in buckling response of the orthogrid panel. Such a modeling approach reduces the number of elements from 2280 to 1020, and provides essentially the same results as the large finite element model for this orthogrid panel problem. The constitutive properties of the intersection region are obtained using a detailed finite element model of the cut-and-add region and are listed in Table 2 for different sizes of stiffener discontinuity.

The finite element analysis of orthogrid panels with stiffness discontinuities is performed using the DIAL[9] finite element code. DIAL is a well-evaluated special purpose finite element code developed by Lockheed Missiles and Space Company. The orthogrid panel has an overall length of 152.4 cm (60 in.) and a width of 91.5 cm (36 in.). The stiffener has a rectangular cross section with a height of 3 cm (1.2 in.) and a width of 0.762 cm (0.3 in.). With clamped boundary conditions along the transverse edges and simple-support conditions along the longitudinal edges of the panel, the typical buckling mode shape has two longitudinal half-waves and one transverse half-wave. The reductions in buckling resistance obtained for the combined loading case for different sizes of stiffener discontinuities using bifurcation buckling analysis are shown in Fig. 3. The buckling load of the panel with stiffener discontinuities, nondimensionalized by the buckling load of the panel without discontinuities, is plotted in this figure as a function of the discontinuity size expressed as a percentage of the stiffener width t. The maximum discontinuity considered is 0.508 cm (0.02 in.), which is expected to be the largest discontinuity associated with an automated manufacturing environment. Manufacturing-introduced stiffness discontinuities due to the cut-and-add approach seem to have a very small influence on

Table 1 Nominal mechanical properties for AS4/3501-6 graphite epoxy unidirectional material

Longitudinal modulus, GPa (Msi)	137.8 (20.00)
Transverse modulus, GPa (Msi)	11.3 (1.64)
In-plane shear modulus, GPa (Msi)	6.0 (0.87)
Major Poisson's ratio	0.30

Table 2 Smeared constitutive properties of stiffener intersection region

Property	Stiffener discontinuity size, cm (in.)			
	0.000 (0.000)	0.0127 (0.005)	0.0254 (0.010)	0.0508 (0.020)
Longitudinal modulus, GPa (Msi)	68.9 (10.00)	67.6 (9.813)	65.6 (9.518)	61.80 (8.972)
Transverse modulus, GPa (Msi)	68.9 (10.00)	67.6 (9.813)	65.6 (9.518)	61.80 (8.972)
In-plane shear modulus, GPa (Msi)	6.0 (0.870)	5.71 (0.829)	5.4 (0.783)	4.75 (0.690)
Major Poisson's ratio	0.0500	0.0498	0.0496	0.0494

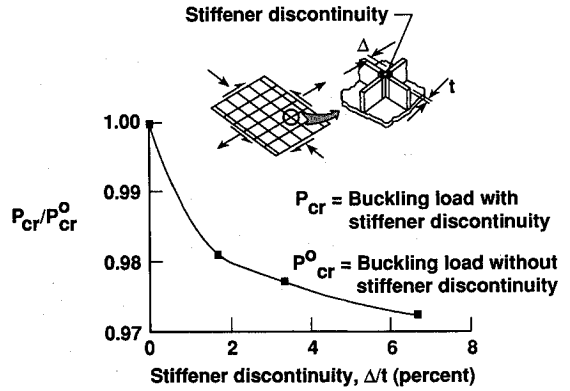

Fig. 3 Effect of stiffener discontinuity size on the buckling resistance of orthogrid panel.

the buckling resistance of the orthogrid panel studied. The degradation in buckling resistance is about 3% for a stiffener discontinuity of 0.0508 cm (0.02 in.).

Effect of Induced Damage on Isogrid Panels

Isogrid structures are considered to be damage-tolerant due to a multiplicity of load paths provided by the stiffener grid. For this reason, even if part of the grid is damaged, enough load paths exist for the panel to sustain the loading. In Ref. 5, damage tolerance of isogrid panels was demonstrated by severing the stiffener elements progressively to simulate each damage case and then testing them for buckling resistance. These results correlated well with finite element results suggesting that the model adequately predicted damaged-panel buckling behavior. In the present article, finite element analysis of damaged panels is performed in a similar manner to generate quantitative information for isogrid stiffened panels with simply-supported boundary conditions and combined loading conditions.

The isogrid panels studied herein have simply-supported boundary conditions on all edges. The behavior of these panels is examined for uniaxial compression, combined compression, and shear loading cases. Two isogrid panels are designed, one to carry a uniaxial compression loading of 525 kN/m (3000 lb/in.) and the second to carry a combination of 525 kN/m (3000 lb/in.) axial compression and 105 kN/m (600 lb/in.) shear loading, at buckling. A typical mode shape of these panels without damage is shown in Fig. 4a. The shaded region of the panel shown in Fig. 4b is modeled so that individual stiffener elements in this part of the panel could be removed in order to simulate different damage cases and to study degradations in the buckling resistance of the panel. This approach is taken because damage in locations of maximum bending strains has the greatest influence on the buckling load of these types of panels. In this study, only damage to stiffeners shown as thick lines in the shaded region is considered. Details of the damage cases for which results are generated are illustrated in Fig. 5. The dashed lines in each damage case represent the stiffeners that are virtually eliminated from the finite element model to simulate damage by reducing their mechanical properties to a small value. The degradation of buckling resistance for each damage case is presented in Fig. 6 where the buckling load of the panel with simulated damage (P_{cr}) is nondimensionalized by the buckling load of the undamaged panel (P^{0}_{cr}).

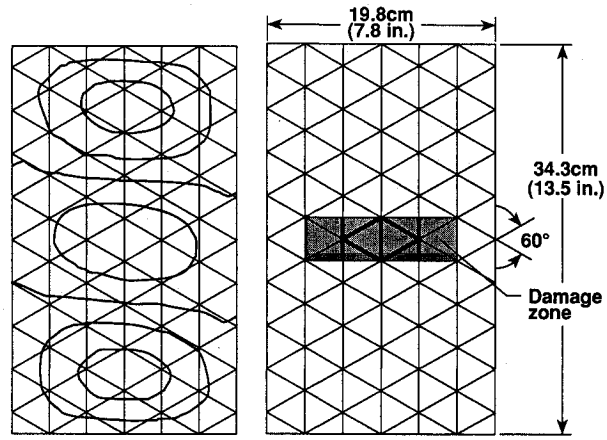

Fig. 4 Typical buckling mode shape and the damage zone for isogrid panels.

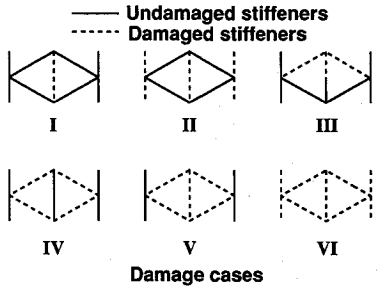

Fig. 5 Damage cases for study.

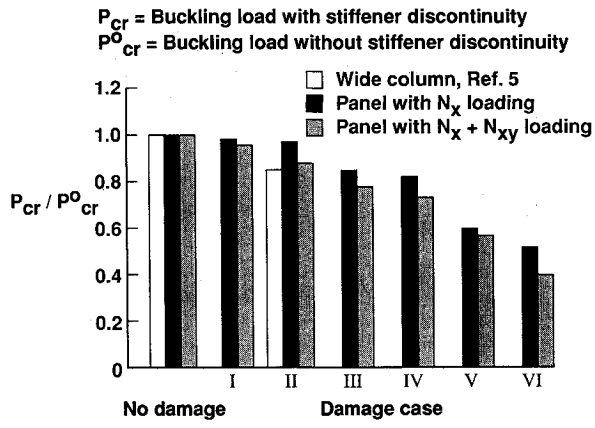

Fig. 6 Effect of induced damage on the buckling resistance of isogrid panels subjected to uniaxial and combined loading.

The degradation of buckling resistance for an isogrid wide column (Ref. 5) is also plotted in Fig. 6 for comparison with the present results.

The buckling mode shapes for simply-supported isogrid panels subjected to combined loading conditions are presented for different damage cases in Fig. 7. These are global buckling mode shapes resulting from damage at local regions. For example, damage to one stiffener segment in the center, cor-

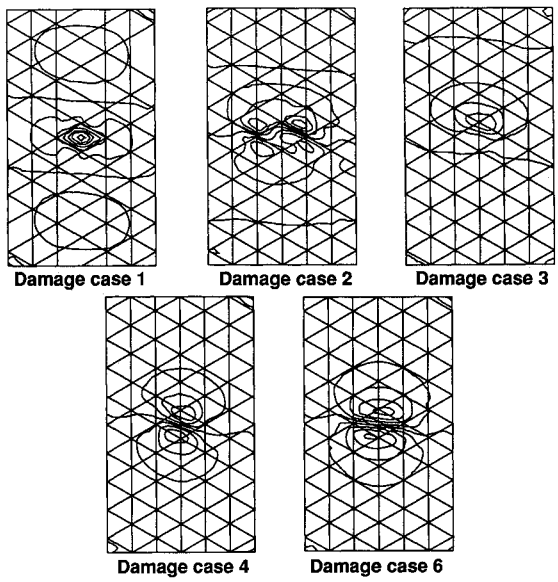

Fig. 7 Mode shapes for damaged isogrid panels subjected to combined loading.

responding to damage case 1 in Fig. 5, results in local buckling of the diamond skin panel, while the global mode constituting three longitudinal half-waves is maintained. For other damage cases, however, there is a considerable change in the buckling mode shapes, depending on the extent and nature of damage.

For the uniaxially loaded, simply-supported isogrid panels, the effect of damaging only the longitudinal stiffeners on the buckling resistance of the panel is small; the reduction in buckling resistance is less than 4% with damage to three longitudinal stiffeners (damage case 2). The load in the panel is redistributed to the diagonal stiffeners in this case. Damage to both the longitudinal and diagonal stiffeners results in large reductions in buckling resistance. These degradations are due to the absence of any stiffeners in the damaged zone to redistribute the load, and the local buckling of the large unsupported region inducing the panel to buckle in a global mode. For damage case 5, the reduction is about 43%. The addition of shear loading reduces the buckling resistance of the panel still further. Damage to any stiffening member is critical for this combined loading condition as indicated by the results where the buckling resistance monotonically decreases for the damage cases chosen. The degradation in buckling resistance is 60% for the combined loading condition with damage to all stiffeners in the panel zone selected (damage case 6) which may be representative of a service-induced impact threat.

Studies of Panels with Nonsolid Stiffener Cross Sections

The designs of continuous-filament grid-stiffened structures have used only the solid blade cross sections shown in Fig. 2 so far. Some other cross sections that may be more efficient and manufacturable with equal ease compared to the solid-blade cross sections, are foam-filled blade and foam-filled hat sections illustrated in Fig. 2.

Grid-stiffened structures using foam-filled stiffeners are constructed utilizing the same manufacturing procedure as used for the solid blade panels. The overwrap material (see Fig. 2) is first placed in a female tool and the unidirectional material is filament-wound in place to form a 0-deg material cap. A premachined Rohacell/syntactic foam material insert is next placed in the tool to complete the stiffener. The skin material is then filament-wound to the required thickness to complete the assembly which is cured to produce the required grid-stiffened structure. The purpose of the foam material is to provide compacting pressure from the inside of the stiffener during curing and to serve as a support for the stiffener during structural loading. This fabrication procedure has the potential to produce grid-stiffened structures that have varied or tailored stiffnesses in different directions.

Prismatic Stiffener Panels

A design optimization study is carried out to determine the relative efficiencies of prismatically stiffened (longitudinal stiffeners of constant cross section) panels with solid blade, foam-filled blade, and foam-filled hat stiffeners. The foam material used for these design studies is Rohacell WF71 which is a structural foam that can be cured at 350°F. Typical properties of this foam material are presented in Table 3. The panel analysis and sizing code[10] (PASCO) is used for this study. The length of the panel is 76.2 cm (30 in.) and the width is 61 cm (24 in.). A stiffener spacing of 15.24 cm (6 in.) is chosen for a panel for four stiffeners. All panels are simply-supported along the edges. The results are presented as structural efficiency curves in Fig. 8 where the weight index W/AL of the panels are plotted against the load index N_x/L, where W is the weight, L is the length, A is the area, and N_x is the stress resultant in the x direction. These results indicate that the foam-filled hat cross section is structurally superior to the two blade cross sections at all load levels. This foam-filled concept is 15–25% lighter than the more conventional solid blade concept in the 525–3500 kN/m (3000–20,000 lb/in.) load range considered. The foam-filled blade cross section is comparable to the solid-blade cross section in the 525–1050 kN/m (3000–6000 lb/in.) load range, but is more efficient at higher load levels. If grid-stiffened panels for combined load applications have stiffeners of the same dimensions placed in all directions, the foam-filled blade concept may be more efficient than the solid blade cross section in this load range. To explore this possibility, the following study was conducted for an orthogrid panel subjected to a combined loading condition that is typical of transport aircraft fuselage structure.

Orthogrid Panels

The design loading of the orthogrid panel is 525 kN/m (3000 lb/in.) compression in the longitudinal direction, 263 kN/m (1500 lb/in.) tension in the transverse direction, and an in-plane shear of 105 kN/m (600 lb/in.). The solid blade stiffener panel is designed using a grid-stiffened panel sizing procedure that uses local and global buckling constraints. This design was verified using finite-element analysis results from the DIAL finite-element code. A finite-element-based design study was then performed to size a foam-filled blade orthogrid panel

Table 3 Nominal properties for Rohacell WF71 foam material

Longitudinal modulus, MPa (ksi)	90.26 (13.10)
Shear modulus, MPa (ksi)	29.42 (4.27)
Poisson's ratio	0.53
Density, kg/m^3 (lb/in.^{3})	70.00 (0.00253)

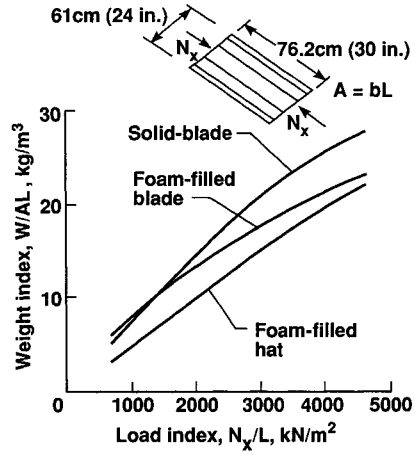

Fig. 8 Structural efficiency results for different stiffener cross sections defined in Fig. 2.

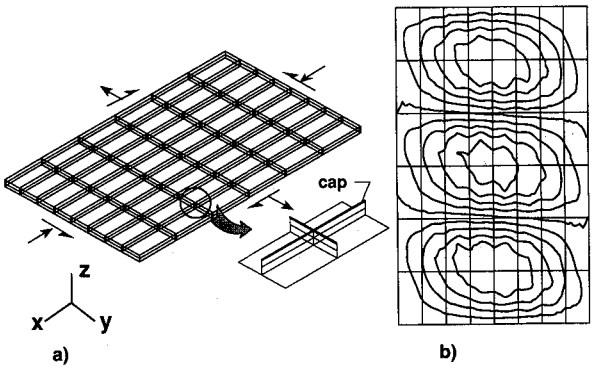

Fig. 9 Finite element model and buckling mode shape of foam-filled blade stiffened orthogrid panel: a) finite element model and b) mode shape.

Table 4 Geometry and stacking sequence for solid and foam-filled blade orthogrid panels

Geometric parameter	Size, cm (in.) Solid blade orthogrid	Foam-filled blade orthogrid
Panel length	152.4 (60.00)	152.40 (60.00)
Panel width	91.5 (36.00)	91.50 (36.00)
Stiffener height	3.3 (1.30)	3.56 (1.40)
Stiffener width	0.508 (0.20)	2.00 (0.79)
Cap thickness	——	0.28 (0.11)
Web thickness[a]	——	0.0508 (0.02)
Skin thickness[b]	0.508 (0.20)	0.508 (0.20)

[a]Web stacking sequence: $(\pm 45)_s$.
[b]Skin stacking sequence: $(45/0_2/-45/0/-45/0/45/90/45)_s$.

that carries the same load as the reference solid-blade panel at buckling. The finite-element model of the orthogrid panel is shown in Fig. 9a where the stiffeners are modeled as plate elements with two different material properties, one corresponding to the foam-filled region and the other to the predominantly 0-deg cap material. The buckling mode shape for this panel is the same as that of the solid-blade panel and is shown in Fig. 9b. The weight of the solid blade panel is 10.26 kg (22.63 lb) which is 12% heavier than the foam-filled blade panel for the same design loading conditions. This example suggests that although the two concepts are comparable in structural efficiency in a prismatically stiffened panel case subjected to uniaxial compression of 525 kN/m (3000 lb/in.), in a more practical combined loading case, the foam-filled blade concept provides the lighter weight design. The dimensions and stacking sequences of the laminates for the two designs are presented in Table 4.

Elastic Tailoring with Composite Grid-Stiffened Structures

Elastic Tailoring

Elastic tailoring refers to the utilization of the design flexibility of composites to achieve performance goals. The goals are usually accomplished by selecting an appropriate structural concept, fiber orientation, ply stacking sequence, and a blend of materials. Grid-stiffened structural concepts are particularly useful for elastic tailoring of structures because stiffeners of unidirectional material can be oriented to create a wide variation of elastic properties. A concept for altering the effective Poisson's ratio to produce significantly large chordwise camber deformations of wings is outlined in this section. This wing lift enhancing deformation shown in Fig. 10 may be utilized to reduce or modify the requirements for control surfaces like flaps and their associated systems.

Design Application

For one high-aspect ratio wing camber-producing concept, a large effective Poisson's ratio is desired for the wing covers. This can be accomplished by utilizing a stiffener pattern and

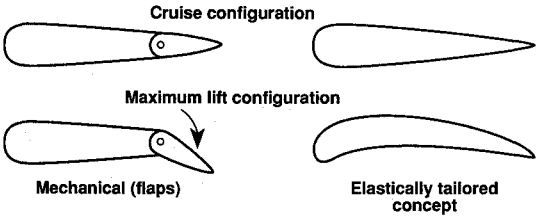

Fig. 10 Mechanisms to enhance lift.

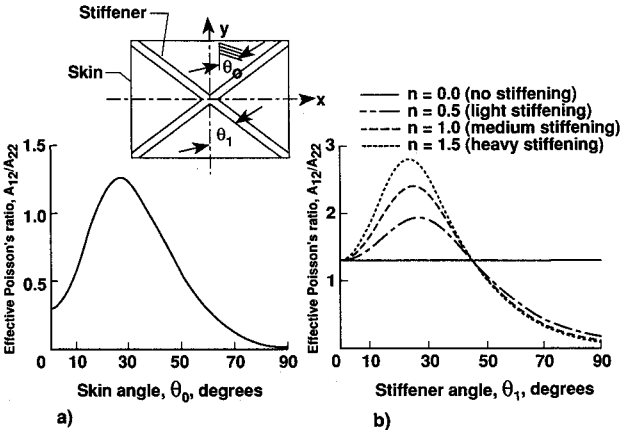

Fig. 11 Effect of skin fiber and stiffener orientation on effective Poisson's ratio: a) effect of skin orientation and b) effect of stiffener orientation (with skin angle $\theta_0 = 26°$).

a balanced skin lay-up as shown in Fig. 11. The spanwise coordinate is denoted by x and the chordwise coordinate by y. The in-plane stress resultants for the wing cover are

$$N_{xx} = A_{11}\varepsilon_{xx} + A_{12}\varepsilon_{yy} \tag{1}$$

$$N_{yy} = A_{12}\varepsilon_{xx} + A_{22}\varepsilon_{yy} \tag{2}$$

$$N_{xy} = A_{66}\gamma_{xy} \tag{3}$$

where ε_{xx}, ε_{yy}, and γ_{xy} are the membrane strains; and A_{11}, A_{12}, A_{22}, and A_{66} are membrane stiffnesses.

If the stiffnesses of the stiffeners are accounted for in an averaged manner, the A_{ij} will be the "smeared" stiffnesses over the area of the panel. These are given by

$$A_{ij} = A_{ij}^0 + A_{ij}^1 \qquad i = j = 1, 2, 6 \tag{4}$$

The superscripts 0 and 1 refer to the skin and stiffener stiffnesses, respectively. For the laminated composite skin, these stiffnesses are obtained using classical lamination theory. For the stiffeners modeled as one-dimensional elements, the membrane stiffnesses are given by

$$\begin{aligned} A_{11}^1 &= 2hnE_{11}^1 \cos^4\theta_1 \\ A_{12}^1 &= 2hnE_{11}^1 \sin^2\theta_1 \cos^2\theta_1 \\ A_{22}^1 &= 2hnE_{11}^1 \sin^4\theta_1 \end{aligned} \tag{5}$$

where E_{11}^1 is the extensional modulus of the stiffeners, h is the skin thickness, n is a stiffening parameter, and θ_1 is the inclination of the stiffener to the x direction. The stiffening parameter n is defined as

$$n = A_1/p_1 h \tag{6}$$

where A_1 is the cross-sectional area of an individual stiffener, and p_1 is the distance between stiffeners.

By virtue of high-aspect ratio wing geometry, the chordwise stress resultant N_{yy} is small and will be ignored. Therefore,

Eqs. (1) and (2) are reduced to the form

$$\varepsilon_{yy} = -(A_{12}/A_{22})\varepsilon_{xx} \tag{7}$$

$$N_{xx} = K_{11}\varepsilon_{xx} \tag{8}$$

where

$$K_{11} = A_{11} - A_{12}^2/A_{22} \tag{9}$$

K_{11} is the effective extensional membrane stiffness, and A_{12}/A_{22} is the effective Poisson's ratio which may be related to the camber. The camber curvature κ_{yy} is given by

$$\kappa_{yy} = -(A_{12}/A_{22})\kappa_{xx} \tag{10}$$

where κ_{xx} is the spanwise curvature.

The ability of the structural concept to enhance the effective Poisson's ratio is illustrated below. Material properties utilized in this study are given in Table 1. A preliminary study of the effects of skin fiber orientation for balanced angle piles on the effective Poisson's ratio is shown in Fig. 11a. These results indicate that a skin orientation angle θ_0 of 26 deg is optimum for the material system selected. Only $\pm\theta$ skin fiber orientations are considered in this illustration. In general, 0- and 90-deg piles may be added without significantly altering the Poisson's ratio. The addition of 0-deg piles produces designs that are structurally more efficient since the dominant load component is in the spanwise direction of the wing.

The influence of adding stiffeners to the skin on the effective Poisson's ratio is illustrated in Fig. 11b. These results are for a skin orientation angle of 26 deg and four different values of the stiffening parameter n [see Eq. (6)]. The values for n equal to 0.0, 0.5, 1.0, and 1.5 correspond to the no stiffening, light stiffening, medium stiffening, and heavy stiffening cases, respectively. For a heavily stiffened panel ($n = 1.5$), the value for the effective Poisson's ratio is about 2.8. These results illustrate the effectiveness of utilizing grid-stiffened structural concepts in elastic tailoring applications.

Concluding Remarks

A numerical study that investigates the effects of stiffness discontinuities, stiffener cross sections, and stiffener orientations on the behavior of grid-stiffened panels has been presented. Two types of stiffness discontinuities have been considered, one due to the cut-and-add manufacturing process that results in very localized reductions in stiffness, and the second due to induced damage to the stiffening members. The reduction in buckling resistance corresponding to the cut-and-add approach-introduced maximum stiffener discontinuity size of 0.0508 cm (0.02 in.), has been determined to be about 3%. This result indicates that the cut-and-add manufacturing method is a viable approach to avoiding the fiber clustering problem in grid-stiffened structures. The tolerance of isogrid panels to induced damage is a function of both panel boundary conditions and applied loading. A panel supported on all four edges has better damage tolerance than a panel tested as a wide column. A combined loading condition has been shown to reduce the damage tolerance of isogrid panels for all the selected damage conditions evaluated herein, suggesting the need to assess the damage tolerance of structures for actual loading conditions.

Foam-filled hat and foam-filled blade stiffener concepts for grid-stiffened panels have been found to be structurally more efficient than the more conventional solid-blade concept. For a combined axial compression and shear loading application, the orthogrid panel with foam-filled blade stiffeners is lighter than the corresponding solid-blade stiffened orthogrid panel, although both cross sections are equally efficient in an application involving a prismatically stiffened panel subjected to uniaxial compression. Grid-stiffened structural concepts have been shown to be very effective in creating large values of effective Poisson's ratio that may be utilized to produce chordwise camber deformations and, therefore, enhanced lift in elastically tailored wing applications.

References

[1]Rehfield, L. W., Deo, R. B., and Renieri, G., "Continuous Filament Advanced Composite Isogrid: A Promising Structural Concept," *Fibrous Composites in Structural Design*, Plenum Press, New York, 1980, pp. 215–239.

[2]Reddy, A. D., "Behavior of Continuous Filament Advanced Composite Isogrid Structure," Ph.D. Dissertation, Georgia Inst. of Technology, Atlanta, GA, Nov. 1980.

[3]Rehfield, L. W., Reddy, A. D., Yehezkely, O., and Armanios, E. A., "Buckling of Continuous Filament Composite Isogrid Panels: Theory and Experiment," *Progress in Science and Engineering of Composites*, ICCM-IV, Tokyo, 1982, pp. 545–553.

[4]Rehfield, L. W., and Reddy, A. D., "Damage Tolerance of Continuous Filament Composite Isogrid Structures: A Preliminary Assessment," *Composite Materials, Proceedings of Japan-U.S. Conference*, Tokyo, 1981, pp. 471–477.

[5]Reddy, A. D., Haag, R., Widmann, C. G., and Rehfield, L. W., "Compressive Buckling Behavior of Graphite/Epoxy Isogrid Wide Columns with Progressive Damage," *Compression Testing of Homogeneous Materials and Composites*, edited by R. Chair and R. Papirno, American Society for Testing and Materials, STP 808, 1983, pp. 187–199.

[6]Reddy, A. D., Valisetty, R. R., and Rehfield, L. W., "Continuous Filament Wound Grid Stiffened Composite Structures for Aircraft Fuselages," *Journal of Aircraft*, Vol. 26, No. 2, 1985, 249–255.

[7]Phillips, J. L., "Structural Analysis and Optimum Design of Geodesically Stiffened Composite Panels," M.S. Thesis, Virginia Polytechnic Inst. and State Univ., Blacksburg, VA, Feb. 1990.

[8]Anderson, R. G., "Manufacturing of the Army/Bell Advanced Composite Helicopter Airframe," *Proceedings of the American Helicopter Society, Composite Structures Specialist's Meeting*, Philadelphia, PA, March 23–25, 1983.

[9]DIAL Finite Element Analysis System—Version L3D2. Lockheed Missiles and Space Co. Inc., Sunnyvale, CA, July 1987.

[10]Stroud, W. J., and Anderson, M. S., "PASCO: Structural Panel Analysis and Sizing Code, Capability and Analytical Foundations," NASA TM-80181, Nov. 1981.